NANO LETTERS

2007
Vol. 7, No. 2
520−524

Charge-Induced Rayleigh Instabilities In Small Gold Rods

Carolina Novo and Paul Mulvaney*

School of Chemistry, University of Melbourne, Parkville, VIC 3010, Australia

Received November 12, 2006; Revised Manuscript Received December 15, 2006

ABSTRACT

It is demonstrated that the addition of electrons to gold nanorods with aspect ratios ranging from 2 to 4 leads to an initial blue-shift in the absorption spectrum due to the increasing surface plasmon frequency of the electron gas. However, at longer times, there are changes in particle morphology induced by the surface charge. In the case of smaller injected electron densities, the surface plasmon band red-shifts as the end caps of the rods undergo increased faceting and develop {111} faces. In the case of higher electron densities, the rods undergo fragmentation into clouds of smaller spheres. These secondary processes and fragmentation are postulated to be a direct result of crossing the Rayleigh threshold.

Introduction. The mechanical stability of small metal rods and wires is an important consideration when assessing their potential utility in optical, electronic, or sensing devices. There is increasing evidence that such nanoscale metal structures are far more vulnerable to damage by heat and light than the respective bulk metals. For example, metal nanowires heated inside an electron microscope have been found to spontaneously fragment at temperatures well below the melting point.[1] This mechanical break-up was attributed to thermally induced surface oscillations. Such oscillations can lead to mechanical instability, even below the melting point of the bulk. They are well-known in liquid drops and are termed Rayleigh instabilities.[2] Kamat and Hartland have reported fragmentation of small metal particles in aqueous solution following intense pulsed laser excitation. A similar mechanism may be operative in that case because excitation of the surface plasmon modes causes rapid expansion of the particle, which in turn launches large-amplitude, acoustic oscillations, which can be observed by picosecond transient spectroscopy.[3] In both of these cases, the changes in particle morphology were induced by thermal fluctuations.

Another common method for imposing instability on a liquid droplet is through electrical charging. In this case, the cohesive force provided by the surface tension is offset by the electrical stress created by the surface charge distribution. This effect has also been studied in detail by Rayleigh, who analyzed the mechanical stability of liquid spheres in the presence of electrical charges.[4] A transient jet or Taylor cone is often observed just prior to break-up.[5] These effects have been analyzed in more detail recently because of the importance of the phenomenon in electrospray mass spectrometry. Li et al. have extended the macroscopic continuum model for charge stability down to micron-sized droplets suspended in an electrodynamic balance,[6] while Smith and co-workers have demonstrated conclusively that small liquid droplets rapidly disintegrate upon external charging and that the critical mass:charge ratio is accurately given by the Rayleigh equation:[7]

$$Q = 8\pi(\epsilon_o \gamma a^3)^{1/2} \quad (1)$$

where Q is the charge on the sphere, a is the sphere radius, γ is the surface tension, and ϵ_o is the permittivity of the surroundings.

To date, there have been no studies of charge-induced Rayleigh instabilities in small, *solid* particles. This is partly because of the experimental difficulty in applying significant charge to fine, suspended particles and the expected slow response time of such a solid to the induced stress. It is also difficult to quantify and monitor the likely small changes in the surface morphology that would ensue from any induced mechanical instabilities. In particular, if the resultant changes in morphology were elastic and the particle recovered from the applied stresses, direct observation would be exceedingly difficult.

In this paper we report for the first time clear evidence that nanoscale metal rods will undergo shape changes in response to double-layer charging. Nanoscale metal particles provide a useful system for studying the importance of Rayleigh instabilities. First, the particles have well-defined crystal structures and geometries, which can be investigated by electron microscopy at the atomic level. Second, even minor changes to the particle geometry and charge may lead to discernible optical shifts in the surface plasmon absorption band, which may consequently be used to monitor such

* Corresponding author. E-mail: mulvaney@unimelb.edu.au.

10.1021/nl062649t CCC: $37.00
Published on Web 01/06/2007

morphological changes in real time.[8−14] In this paper, we will show that electrostatic charging does indeed cause mechanical instabilities in small metal particles and that this results in shape changes to the rods. Furthermore, in severe cases, fragmentation occurs and is fast enough to compete with redox reactions that would discharge the double layer.

The gold nanorods used in these experiments were synthesized chemically, following the seed-mediated growth methods developed by Nikoobakht. et al.[15] and Jana et al.[16] Briefly, gold seeds were prepared by adding 5.0 mL of 0.00050 M $HAuCl_4$ to 5 mL of a 0.2M CTAB solution. Ice-cold $NaBH_4$ (0.6 mL) was added to the solution while stirring. A gold nanorod growth solution was prepared by adding 5 mL of 0.001M $HAuCl_4$ to 5 mL of 0.2M CTAB. To this mixture, different amounts of 0.004M $AgNO_3$ solution were added (0.05−0.25 mL), followed by the addition of 0.07 mL of 0.0788 M ascorbic acid. Finally, 0.012 mL of seed solution was added. The reaction took approximately 1 h. Increasing concentrations of $AgNO_3$ led to higher aspect ratio nanorods. The solutions used were approximately one week old. No cleaning processes were used because initial experiments showed that removing excess reagents did not alter the results. The TEM samples were prepared by addition of a drop of solution onto a carbon-coated copper grid. This drop was dried 5 min afterward.

Shape Changes. Electron transfer from ascorbic acid (AA) to gold nanorods was studied by adding different amounts of AA to nanorod solutions of four different aspect ratios: 2, 2.5, 3, and 4. Ascorbate anions were added at concentrations of 1.0, 5.0, and 50 mM, while the gold ion concentration was kept constant at 0.5 mM. After the addition, the optical extinction spectra were collected every 2 min for 10 min, then every 10 min, and then every day after that for approximately 10 days. It is well-known that the optical properties of nanoparticles are size- and shape-dependent. In the case of nanorods, two extinction bands are present in the visible part of the spectrum due to longitudinal and (doubly degenerate) transverse oscillations of the conduction electrons. The peak wavelength of the longitudinal surface plasmon resonance, in particular, is very sensitive to the rod aspect ratio and shifts to longer wavelengths as the aspect ratio increases. The transverse band is not very sensitive to the aspect ratio and furthermore is in the same spectral region as the single surface plasmon mode of gold spheres. Consequently, this absorption band is less useful for monitoring shape changes in the solution.[17−20]

In all samples, after the addition of ascorbic acid, the spectrum underwent an abrupt blue-shift. However, thereafter, the band underwent a red-shift that continued for an hour or two. The surface plasmon band did not recover to its initial position, as is clear from Figure 1.

The trend (blue-shift then red-shift) was observed for rods of all aspect ratios, indicating the process is independent of the particle aspect ratio. Increasing the concentration of ascorbic acid did however lead to greater initial blue-shifts and subsequent red-shifts. In Figure 2, low-resolution electron microscope images of gold nanorods of aspect ratio 4 are shown before (a) and after addition of (b) 1 mM and (c) 50 mM ascorbic acid.

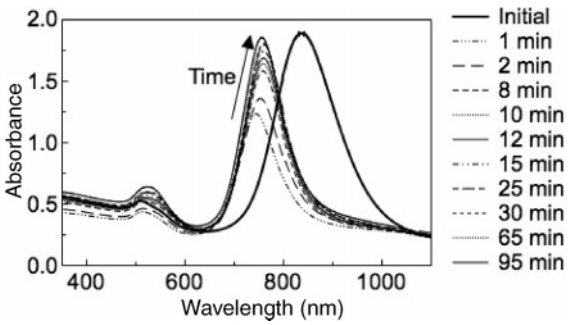

Figure 1. Longitudinal plasmon band blue-shifting and then red-shifting after the addition of 1 mM ascorbic acid to a solution containing gold nanorods ($[HAuCl_4] = 0.5$ mM) of aspect ratio 4.

If ascorbic acid concentrations of up to 1 mM were added, then the hemispherically capped gold rods were converted to pure cylinders, that is, the hemispherical endcaps became flatter (compare parts a and b of Figure 2). This was found for rods with aspect ratios ranging from 2 to 4. If higher concentrations of ascorbic acid were employed, quite different morphological changes occurred and the endcaps of the nanorods became pointed and there was clear growth of the endcaps as well as a thinning of the waist of the gold rod body (Figure 2c).

High-resolution TEM images of the endcaps of the particles before and after shape changes enable these electrostatically induced changes to be seen in more detail (Figure 3).

It is also important to point out that when the hemispherically capped nanorods were converted to nanocylinders, their average aspect ratio decreased. This suggests that the gold on the end of the rods is moving from the {100} face toward the {110} and {111} faces. There were no large scale changes in the metal crystal structure. The rods remained as single crystals with the same bulk lattice constants. The transfer of electrons to the rods appeared to affect only the faceting of the rods, with the {111} facet becoming more predominant. This is the lowest energy facet for fcc gold.

Fragmentation. Sodium borohydride is a very powerful chemical reductant, which is unstable in water and slowly decomposes, forming hydrogen. Borohydride anions were added to the rod solutions at concentrations of $2\cdot10^{-6}$, $2\cdot10$, $2\cdot10^{-4}$, 0.5, 2.5, and 5 mM. The gold concentration in the nanorod solutions was kept constant at 0.5 mM. After the addition, the reactions were monitored by changes to the optical extinction spectra of the solutions. For the three lower $NaBH_4$ concentrations, $2\cdot10^{-6}$, $2\cdot10^{-5}$, and $2\cdot10^{-4}$ mM (where ratio the $NaBH_4$:Au was approximately 10^{-6}:1, 10^{-5}:1, and 10^{-4}:1, respectively), no detectable changes were observed in the spectra of the solutions, indicating that no significant charging occurred because an increase in electron density would lead to perceptible blue-shifts in the absorption spectrum. This may be partly due to rapid decomposition of borohydride to form H_2 in low concentrations. More concentrated solutions of $NaBH_4$ decompose more slowly.

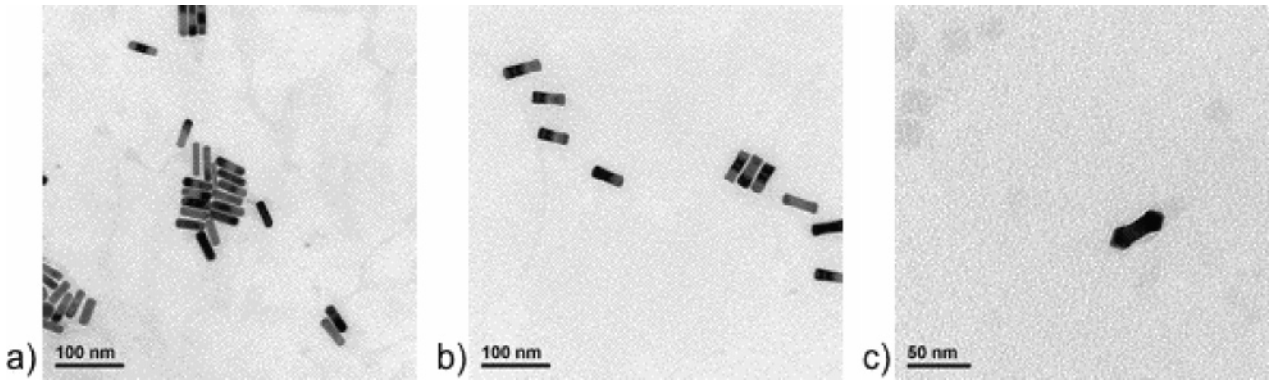

Figure 2. Electron micrographs of gold nanorods of aspect ratio 4 (a) as synthesized, and after addition of (b) 1 mM and (c) 50 mM ascorbic acid.

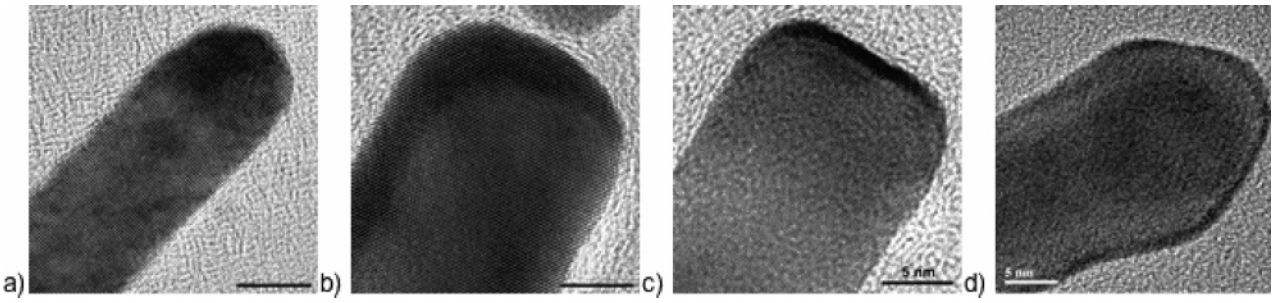

Figure 3. HRTEM images of the end caps of nanorods of initial aspect ratio 4, (a) before and after addition of (b, c) 1 mM and (d) 50 mM ascorbic acid. Scale bar is 10 nm in the first image and 5 nm in (b−d).

At higher $NaBH_4$ concentrations, where the ratios of $NaBH_4$ molecules to gold nanorods were 1:1, 10:1, and 100:1, the spectrum blue-shifted rapidly after the addition, and then more slowly for an hour. However, further slow changes continued for up to 10 days after mixing. These changes can be seen for a solution of nanorods of aspect ratio 4 in Figure 4. The same trend was observed for nanorods of aspect ratio 2, 2.5, and 3. At the same time as these changes to the SPL band occurred, the transverse band increased greatly in intensity. The SPL band did not return to its initial position, and a permanent increase in the intensity of the transverse band was also seen.

In all cases, the longitudinal band blue-shifted immediately after the addition of sodium borohydride and kept shifting for about 10 days. The transverse band increased in intensity greatly. Increasing concentrations of borohydride caused the longitudinal band to blue-shift to increasingly shorter wavelengths. Thus the final surface plasmon band peak position was shorter for rods containing higher concentrations of $NaBH_4$.These results are quite different to those obtained with the weaker reductant, ascorbic acid, where the initial blue-shift was followed by a red-shift. Figure 5 (a and b) shows electron microscope images of the nanorods of aspect ratios 4 as synthesized, and (c and d) after addition of 5 mM $NaBH_4$.

Initially, only rods were observed by electron microscopy. After sodium borohydride was added, fewer rods were found, and these exhibited a wide variety of aspect ratios. In addition, a large fraction of the particles consisted of very small spheres (1−3 nm diameter). The spectral changes are consistent with both a decrease in the aspect ratio of the gold rods over time, which causes the longitudinal mode to decrease and blue-shift, while the appearance of small spheres is evident from the enhancement of the plasmon band at 520 nm, which is the peak position in water for small gold spheres.

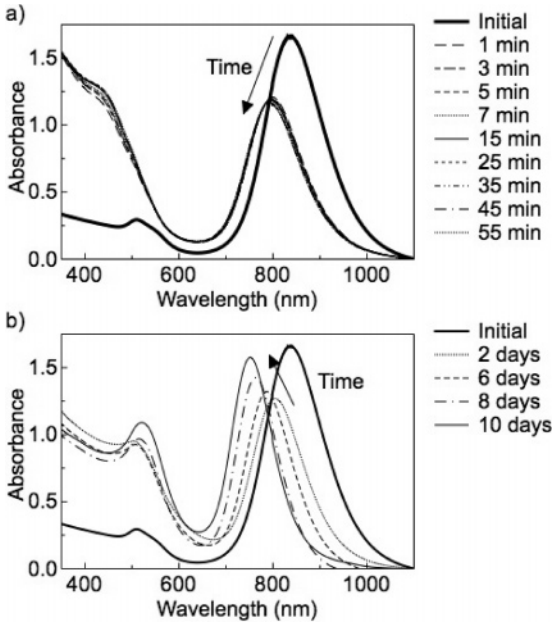

Figure 4. Spectra of a solution of gold nanorods ($[HAuCl_4]$ = 0.5 mM) as a function of time after the addition of 5 mM $NaBH_4$: (a) over an hour (b) over 10 days.

Reversibility and Reactivation. To test the reversibility of the reaction, one of the samples (aspect ratio 4, [AA] = 1.00

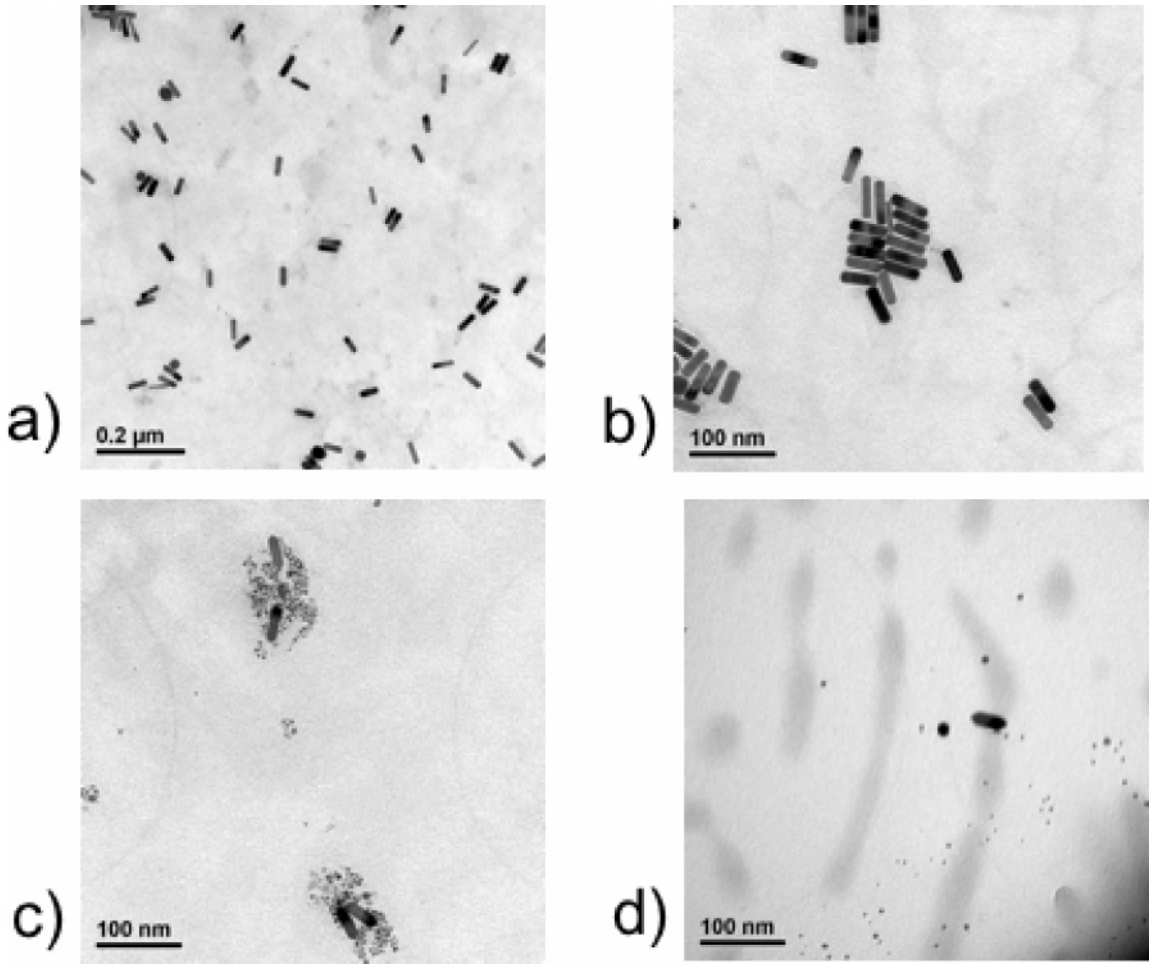

Figure 5. (a and b) Gold nanorods ([$HAuCl_4$] = 0.5 mM) of aspect ratio 4 before addition of sodium borohydride showing almost exclusively rods well dispersed on the grid; (c and d) after addition of 5 mM $NaBH_4$, showing the rods surrounded by gold spheres around 3−10 nm in size.

mM) was observed over time. First, TEM images were acquired on the day of the reaction, and the particles shown in Figure 4a were observed. This same sample was left for 10 days, and a new TEM grid was prepared and analyzed. The particles were unchanged and did not convert back to the initial hemispherical endcapped shape. This indicates that the reaction observed is irreversible and the shape changes occurring to the nanorods lead to plastic deformation.

Discussion. For small metal ellipsoids, the surface plasmon modes will blue-shift when the electron density in the particle increases by an amount ΔN, with the wavelength shift from an initial peak wavelength λ_o being given by:

$$\Delta\lambda = \lambda - \lambda_o = -\frac{\Delta N}{2N}\sqrt{\epsilon_\infty + \left(\frac{1}{L} - 1\right)}\epsilon_m \qquad (2)$$

Here N is the conduction electron density, L the depolarisation factor, which is dependent upon the shape of the particle, ϵ_∞ is the high-frequency dielectric constant of gold and ϵ_m is the dielectric constant of the nonabsorbing medium. Equation 2 predicts a blue-shift in the spectra of rods and spheres and is seen whenever reductants are added to small (silver or) gold metal particles.[10] However, the subsequent red-shifts have usually been assumed to indicate a slow discharge of the excess electrons on the gold particles by oxygen or water molecules. The results presented here clearly demonstrate that these slower red-shifts are due, at least in part, to restructuring of the gold nanocrystals. Recent DDA calculations by Prescott et al. show that the depolarisation factor, L, for a flat cylinder is smaller than that for a hemispherically capped rod of the same overall aspect ratio.[21] Thus the observed red-shift is also consistent with the electron microscopy results because the conversion from hemispherical to flat endcap will lead to a red-shift in the surface plasmon absorption band.[22] The question that arises is whether the surface charge densities necessary to induce Rayleigh instabilities and fragmentation can be generated by simple chemical charging of the gold nanorod double layer. Quantification of the threshold for Rayleigh instabilities of nanorods in water is more complicated than for liquid drops in air for several reasons. First, the crystals exhibit several different crystal facets so the surface tension varies over the crystal surface. Furthermore, the differences in work function of the different facets will result in different surface charge densities on each surface. Third, the surface energy is lowered by the adsorption of surface charge and the

formation of the double layer through the well-known Lippmann equation. Finally, the double-layer capacitance is a sensitive function of the electrolyte concentration, the particle radius, and the surface potential. For high potentials, the capacitance may be approximated by a constant Helmholtz capacitance, K_I, which for the gold−water interface is about 0.080 F/m^2. As a first approximation, we estimate the critical surface potential for Rayleigh instabilities in a small sphere in a solvent to be

$$\phi = \frac{2(\epsilon_r \epsilon_o \gamma)^{1/2}}{K_I a^{1/2}} \quad (3)$$

Inserting $\epsilon_r = 78.5$, $\gamma = 0.2$ N m^{-1}, $K_I = 0.08$ F m^{-2}, and an effective radius $a = 4 \times 10^{-8}$ m yields a threshold surface potential of about ±1 V. Given that the standard redox potential of $NaBH_4$ is about −1.2 V NHE and the open circuit potential of metal particles in aqueous solution is around +0.1 V NHE, it seems likely that strong reductants may well lead to surface potentials of order −1 V and hence may induce morphological changes to small metal particles, particularly those with nonequilibrium geometries.

As a corollary to this calculation, it would appear likely that chemical charging would be most likely to drive shape changes for metals with the largest overpotential for hydrogen formation and with the lowest melting points such as copper, silver, or gold. Conversely, platinum and palladium particles, which are excellent catalysts for hydrogen evolution and which have substantially higher melting points, may be less prone to fragmentation.

The shape changes observed in this study result in an increase in the overall area of the particle, and mechanical work is being done on the particle by the applied surface stress. The gold rods are bound by {110} and {010} facets along the rod major axis and are capped by {100} endcaps if flat or a mixture of {100},{111}, and {110} facets if they exhibit hemispherical capping. Charge-induced faceting results in creation of the more stable {111} facets, which have the lowest surface energy and which therefore have the lowest energy of formation. The {111} facets also have the highest work function and therefore the highest surface charge density in aqueous solution when the particle is in equilibrium with a redox couple. The {111} facet is also predominant on spherical gold particles, and this suggests the surface stress is being relieved in a predictable manner by formation of the more stable crystal facets. More curious is the appearance of the sharp edges around the growing {111} facets. The particle electric field is highest at these crystallographic discontinuities, and these may provide hot spots for driving hydrogen evolution; this in turn would catalyze the discharge of the gold nanorod double layer, and such a process constitutes an unusual example of Le Chatelier's principle in action.

In summary, although charge-induced fragmentation is known from gas-phase studies of liquid drops, it has not been previously demonstrated for solids. Our finding that ascorbic acid induces concentration-dependent shape changes to gold rods and that sodium borohydride is capable of inducing fragmentation in small gold rods is consistent with these gas-phase studies and places a stringent upper limit on the mechanical stability of small wires and rods when electrostatically charged. The results demonstrate that the crystal structure and morphology may be controlled by chemical reactions occurring locally on the particle surface as well as by external macroscopic perturbations such as laser-induced heating.

Acknowledgment. C.N. thanks the University of Melbourne for an IPRS scholarship. This work was conducted through ARC grants FF0561486 and DP 0558608.

Supporting Information Available: Figures S1−S11 provide further results of similar experiments carried out with different rod aspect ratios and at different reductant concentrations. This material is available free of charge via the Internet at http://pubs.acs.org.

References

(1) Toimil Molares, M. E.; Balogh, A. G.; Cornelius, T. W.; Neumann, R.; Trautmann, C. *Appl. Phys. Lett.* **2004**, *85*, 5337. Duft, D.; Achtzehn, T.; Müller, R.; Huber, B. A.; Leisner, T. *Nature* **2003**, *421*, 128.
(2) Rayleigh, L. *Philos. Mag.* **1882**, *5* (14), 184.
(3) Kamat, P. V.; Flumiani, M.; Hartland, G. V. *J. Phys. Chem. B*, **1998**, *102*, 3123. Fujiwara, H.; Yanagida, S.; Kamat, P.V. *J. Phys. Chem. B* **1999**, *103*, 2589.
(4) Rayleigh, L. *Philos. Mag.* **1916**, *31*, 17.
(5) Taylor, G. I. *Proc. R. Soc. London, Ser. A* **1964**, *280*, 383.
(6) Li, K. Y.; Tu, H. H.; Ray, A. K. *Langmuir* **2005**, *21*, 3786−3794.
(7) Smith, J. N.; Flagan, R. C.; Beauchamp, J. L. *J. Phys. Chem. A* **2002**, *106*, 9957.
(8) El-Sayed, M. A. *Acc. Chem. Res*. **2001**, *34*, 257.
(9) Templeton, A. C.; Pietron, J. J.; Murray, R. W.; Mulvaney, P. *J. Phys. Chem. B* **2000**, *104*, 564.
(10) Mulvaney, P. *Langmuir* **1996**, *12*, 788.
(11) Baum, T.; Bethell, D.; Brust, M.; Schiffrin, D. J. *Langmuir* **1999**, *15*, 866.
(12) Foss, C. A., Jr.; Hornyak, G. L.; Stockert, J. A.; Martin, C. R. *J. Phys. Chem.* **1994**, *98*, 2963.
(13) Chapman, R.; Mulvaney, P. *Chem. Phys. Lett.* **2001**, *349*, 358.
(14) Yamada, M.; Tadera, T.; Kubo, K.; Nishihara, H. *Langmuir* **2001**, *17*, 2363.
(15) Nikoobakht, B.; El-Sayed, M. A. *Chem. Mater.* **2003**, *15*, 1957.
(16) Jana, N. R.; Gearheart, L.; Murphy, C. J. *Adv. Mater.* **2001**, *13*, 1389.
(17) Brioude, A.; Jiang, X. C.; Pileni, M. P. *J. Phys. Chem. B* **2005**, *109*, 13138.
(18) Kelly, K. L.; Coronado, E.; Zhao, L. L.; Schatz, G.C. *J. Phys. Chem. B* **2003**, *107*, 668.
(19) Pérez-Juste, J.; Pastoriza-Santos, I.; Liz-Marzán, L. M.; Mulvaney, P. *Coord. Chem. Rev.*, **2005**, *249*, 1870.
(20) van der Zande, B. M. I.; Bohmer, M. R.; Fokkink, L. G. J.; Schönenberger, C. Langmuir **2000**, *16*, 451.
(21) Prescott, S. W.; Mulvaney, P. *J. Appl. Phys.* **2006**, *99*, 123504.
(22) Mulvaney, P.; Pérez-Juste, J.; Giersig, M.; Liz-Marzán, L. M.; Pecharromán, C. *Plasmonics* **2006**, *1*, 61.

NL062649T